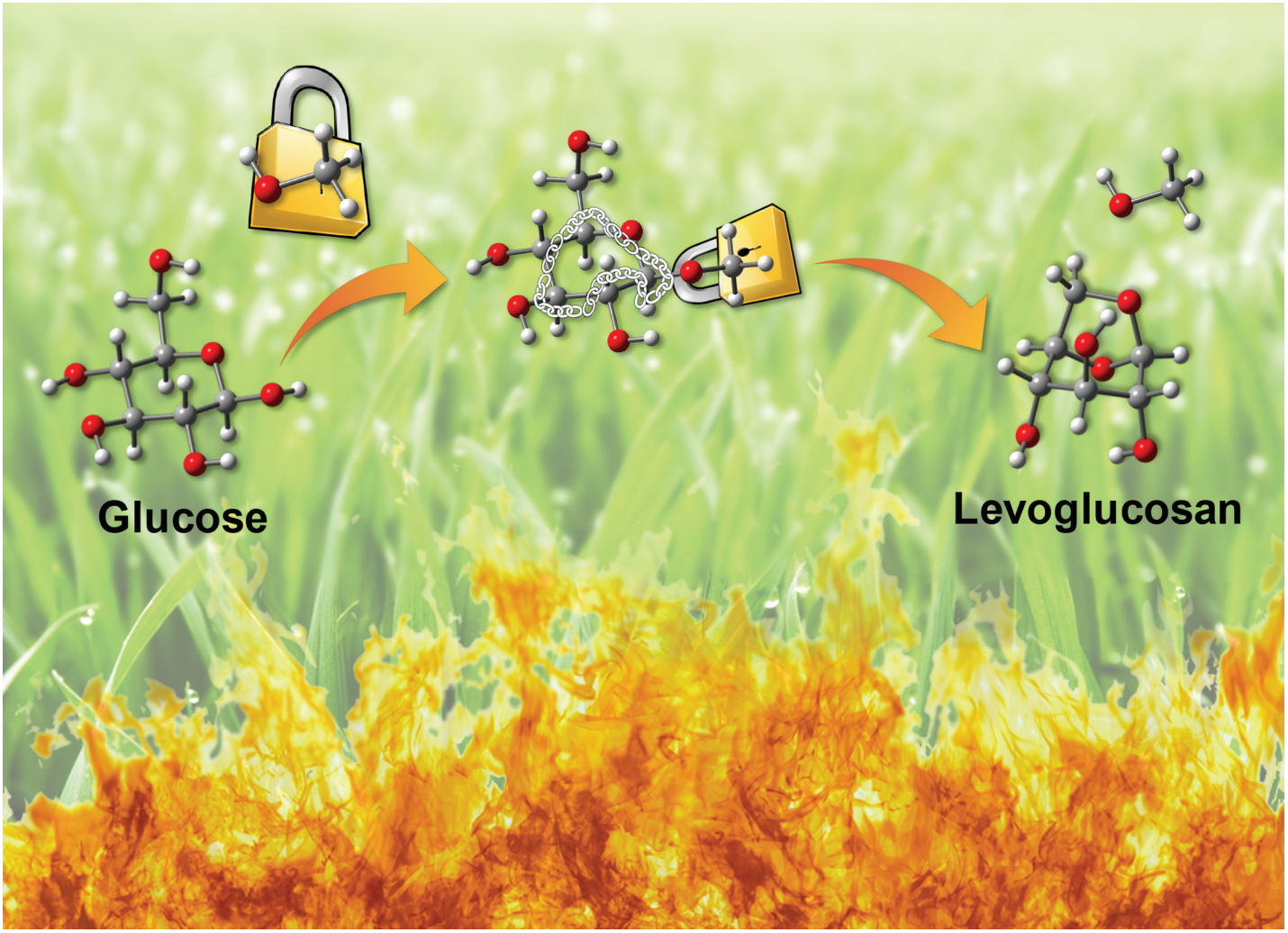

An article presented by the Wong Research Group at Rice University, Texas, USA.

Ring-locking enables selective anhydrosugar synthesis from carbohydrate pyrolysis

Levoglucosan has great potential as a precursor to natural products and drug molecules, but it has been very difficult to manufacture through pyrolysis and other methods. Changing the glucose structure slightly, prior to pyrolysis, prevents the wasteful formation of by-products. The activation barrier to ring-opening (leading to by-products) is raised substantially, which is the basis of the ring-locking effect.

As featured in:

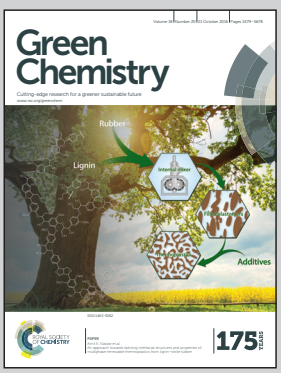

See Z. Conrad Zhang, Michael S. Wong *et al.*, *Green Chem.*, 2016, **18**, 5438.

ROYAL SOCIETY OF CHEMISTRY

www.rsc.org/greenchem

Registered charity number: 207890

Green Chemistry

PAPER

View Article Online
View Journal | View Issue

Cite this: *Green Chem.*, 2016, **18**, 5438

Ring-locking enables selective anhydrosugar synthesis from carbohydrate pyrolysis†

Li Chen,[a] Jinmo Zhao,[b] Sivaram Pradhan,[a] Bruce E. Brinson,[b] Gustavo E. Scuseria,[b] Z. Conrad Zhang*[c] and Michael S. Wong*[a,b,d,e]

Received 13th June 2016,
Accepted 21st July 2016

DOI: 10.1039/c6gc01600f

www.rsc.org/greenchem

The selective production of platform chemicals from thermal conversion of biomass-derived carbohydrates is challenging. As precursors to natural products and drug molecules, anhydrosugars are difficult to synthesize from simple carbohydrates in large quantities without side products, due to various competing pathways during pyrolysis. Here we demonstrate that the nonselective chemistry of carbohydrate pyrolysis is substantially improved by alkoxy or phenoxy substitution at the anomeric carbon of glucose prior to thermal treatment. Through this ring-locking step, we found that the selectivity to 1,6-anhydro-β-D-glucopyranose (levoglucosan, LGA) increased from 2% to greater than 90% after fast pyrolysis of the resulting sugar at 600 °C. DFT analysis indicated that LGA formation becomes the dominant reaction pathway when the substituent group inhibits the pyranose ring from opening and fragmenting into non-anhydrosugar products. LGA forms selectively when the activation barrier for ring-opening is significantly increased over that for 1,6-elimination, with both barriers affected by the substituent type and anomeric position. These findings introduce the ring-locking concept to sugar pyrolysis chemistry and suggest a chemical-thermal treatment approach for upgrading simple and complex carbohydrates.

1. Introduction

Biomass-derived carbohydrates are an abundant but underutilized carbon source for the production of fuels, chemicals and materials.[1–5] Pyrolysis is a widely studied thermal process for carbohydrate conversion,[1] but its usefulness in synthesis chemistry is limited by the low structural stability and high reactivity of carbohydrates.[6] Anhydrosugars are primarily prepared from carbohydrate pyrolysis. Their fixed conformation, protected stereoselectivity, and retention of most of their chemical functionality make these sugar derivatives highly desirable precursors. As a model anhydrosugar, LGA is a chiral building block to antibiotics, antiparasitic agents, and other biologically active compounds.[7–12] It also has strong potential as a sugar-based biorefinery feedstock chemical, with the US Department of Energy identifying it as a top-15 candidate.[13] Found in smoke particles from forest fires,[14] LGA is currently prepared in small quantities by extensive purification from cellulose-derived pyrolysis oil.[1,11,15] Large-scale production of LGA remains elusive.

To address this, we considered the counter-intuitive approach of pyrolyzing glucose. As the constituent sugar monomer of cellulose, glucose is precursor to a growing number of valuable chemicals, such as 5-hydroxymethylfurfural,[16,17] lactic acid,[18] butanol,[19] and γ-valerolactone (GVL).[5] However, glucose pyrolysis generates mostly cracked products and char, with negligible amounts of LGA.[20] In principle, synthesizing pure LGA from glucose pyrolysis can be accomplished by (i) carrying out the dehydration step that leads to intramolecular C_1–O_6 bond formation, (ii) de-selecting the other dehydration pathways, and (iii) avoiding ring-opening of the monosaccharide.

The length of cellulose plays a telling role in LGA formation in pyrolysis: longer chains generated more LGA than shorter ones.[20,21] Mettler *et al.* carefully showed that cellulose with ~130 sugar units yielded 27% LGA after pyrolysis, cellodextrins with 2–6 units yielded ~8–18%, and D-glucose yielded 3%.[20] Longer chains contain a larger proportion of sugar units bound to another unit *via* the β-1,4-glycosidic linkage, from which we conjectured that a substituent group at the C_1 position improves LGA selectivity. In this work, we report that the

[a]*Department of Chemical and Biomolecular Engineering, Rice University, Houston, TX 77005, USA. E-mail: mswong@rice.edu*
[b]*Department of Chemistry, Rice University, Houston, TX 77005, USA*
[c]*Dalian National Laboratory of Clean Energy, Dalian Institute of Chemical Physics, Dalian, Liaoning 116023, China. E-mail: zczhang@dicp.ac.cn*
[d]*Department of Civil and Environmental Engineering, Rice University, Houston, TX 77005, USA*
[e]*Department of Materials Science and NanoEngineering, Rice University, Houston, TX 77005, USA*

†Electronic supplementary information (ESI) available. See DOI: 10.1039/c6gc01600f

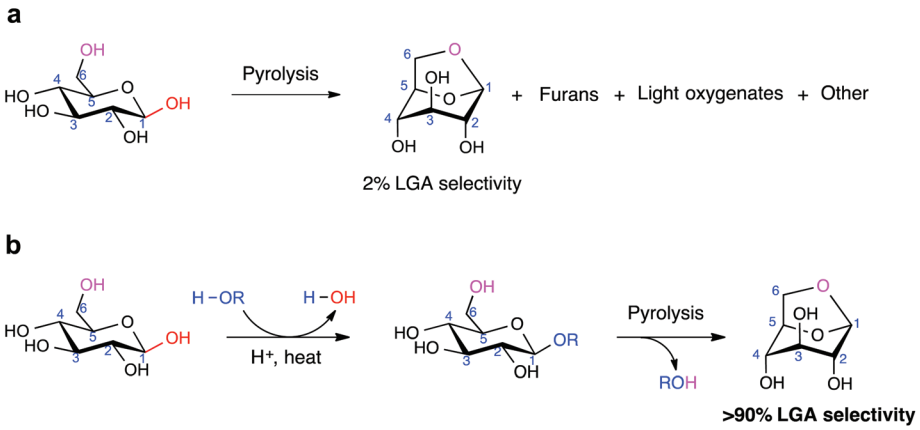

Scheme 1 General schemes of sugar pyrolysis to form levoglucosan ("LGA"). a, Pyrolysis of β-D-glucose ("β-G") leads to LGA after elimination of one water molecule and formation of the 1,6-anhydro bridge, among many other products formed. b, Pyrolysis of functionalized β-G leads to LGA selectively after elimination of ROH.

pyrolysis of β-D-glucose ("β-G") generates LGA with excellent selectivity after its chemical modification at the C_1 position (Scheme 1). Using a combination of flash pyrolysis experiments and density functional theory (DFT) calculations, we show how LGA forms preferentially when ring-opening of the sugar unit is hindered by the presence of the C_1 substituent group and describe how the chemical environment around the C_1 atom impacts 1,6-anhydro bridge formation.

2. Experimental

2.1 Materials

β-D-Glucose (>80.0%, containing α-D-glucose), phenyl-α-D-glucoside (>97%) and methyl-α-D-galactoside (>97% GC) were purchased from TCI America. Methyl-α-D-glucoside (>99%), methyl-β-D-glucoside (>99%), levoglucosan (99%, 1,6-anhydro-β-D-glucose), phenyl-β-D-glucoside (97%), D-mannose (≥99%), D-galactose (>99%) and methyl-α-D-mannoside (≥99% GC) were purchased from Sigma Aldrich. Microcrystalline cellulose was purchased from Alfa Aesar. Other compounds were purchased for column calibrations: DL-glyceraldehyde (>90% GC), glycolaldehyde dimer, furfural (99%), 5-(hydroxymethyl)-furfural (>99%), acetone (>99.9%), and methanol (>99.9%).

2.2 Thin-film for pyrolysis experiments

β-D-Glucose, methyl-β-D-glucoside, and methyl-α-D-glucoside were dissolved into deionized water (18.2 MΩ, Barnstead Nano-pure Diamond System), while phenyl-β-D-glucoside and phenyl-α-D-glucoside were dissolved into 1-propanol : H_2O (1 : 3 by volume) solvent mixture. 4 μL of the solution (8 mg mL^{-1}) was transferred into an open-end cylinder quartz tube (1.9 × 25 mm, diameter × length) by microliter syringe (Hamilton 700 series, 10 μL). Solvent was removed in a vacuum oven at 0.7 atm at 37 °C for 3 h, leading to the formation of a thin-film (containing 32 μg of sugar). The thin-film thickness is determined from Scanning Electron Microscopy (SEM) which is equipped with Energy Dispersive X-ray Spectrometer (EDS) (see ESI for details†). SEM imaging with EDS indicated that the film thickness for all of the samples was less than 10 μm (Fig. S1†).

To confirm appropriate reaction conditions, we followed the analysis of Mettler *et al.*[22] using the Pyrolysis number (Py) and Biot number (Bi) to evaluate our thin-film pyrolysis. Our calculations showed that the thin-film experimentation satisfied the criteria for kinetically limited, isothermal pyrolysis reactions (see the ESI†).

2.3 Pyroprobe coupled with GC/FID system

Thin-films pyrolysis experiments were conducted using a Model 5150 pyroprobe analytical pyrolyzer (CDS Analytical Inc.). The pyrolyzer was coupled to an Agilent 6890N GC/FID through a transfer line for online sampling (Fig. S2, see the ESI† for details of reaction and analysis system). The peaks eluted in the chromatogram was identified by mass spectroscopy, compared with retention time of standard compounds and verified with the previous literatures.[21–23] The GC column was calibrated by injecting standard solution of methanol and phenol into the GC/FID system. LGA was calibrated by evaporating the LGA thin film sample directly through the pyrolyzer upon heating at pyrolysis temperature (600 °C), which appears as a single peak in the GC chromatogram.[21]

2.4 Pyrolysis data evaluation

In order to monitor product distribution of glucose pyrolysis, the yields in this paper are reported in terms of molar carbon yield where the moles of carbon in the product are divided by the moles of carbon in the glucose moiety.

The following equations were used to calculate carbon yield of LGA (Y_{LGA}), conversion of different substrates (X_{sugar}) and selectivity to LGA (S_{LGA}).

LGA carbon yield (Y_{LGA}) for substituted glucose:

$$Y_{LGA} = \frac{\text{moles of carbon in detected LGA}}{\text{initial moles of carbon in glucose moiety}} \times 100\% = \frac{6 \times (\text{moles of detected LGA})}{6 \times \text{initial moles of substituted glucose}} \times 100\% = \frac{\text{moles of detected LGA}}{\text{initial moles of substituted glucose}} \times 100\% \quad (1)$$

LGA carbon yield (Y_{LGA}) from glucose was calculated by the same equation.

We used methanol and phenol as *in situ* generated internal standards to quantify glucoside conversion. Conversion (X_{MG}) for methyl-β-glucoside and methyl-α-glucoside were defined as follows:

$$X_{MG} = \frac{\text{moles of reacted MG}}{\text{initial moles of MG}} \times 100\% = \frac{\text{moles of detected methanol}}{\text{initial moles of MG}} \times 100\% \quad (2)$$

Conversion (X_{PG}) for phenyl-β-glucoside and phenyl-α-glucoside:

$$X_{PG} = \frac{\text{moles of reacted PG}}{\text{initial moles of PG}} \times 100\% = \frac{\text{moles of detected phenol}}{\text{initial moles of PG}} \times 100\% \quad (3)$$

For eqn (2) and (3), we confirmed that (i) methanol/phenol was thermally stable under pyrolysis condition (no side reaction); (ii) methanol/phenol did not react with other pyrolysis products to form ether; and (iii) pyrolysis products did not decompose to form methanol/phenol.

Conversion (X_G) for glucose was quantified using HPLC (details in next section):

$$X_G = \frac{\text{initial moles of glucose} - \text{moles of HPLC detected glucose residue}}{\text{initial moles of glucose}} \times 100\% = \left(1 - \frac{\text{moles of HPLC detected glucose residue}}{\text{initial moles of glucose}}\right) \times 100\% \quad (4)$$

The LGA yield, conversion of starting precursor, and selectivity to LGA were related in the following manner:

$$S_{LGA} = Y_{LGA} \div X_i \quad (5)$$

If i = MG, selectivity to LGA (S_{LGA}) is:

$$S_{LGA} = \frac{\dfrac{\text{moles of detected LGA}}{\text{initial moles of MG}}}{\dfrac{\text{moles of detected methanol}}{\text{initial moles of MG}}} \times 100\% = \frac{\text{moles of detected LGA}}{\text{moles of detected methanol}} \times 100\% \quad (6)$$

If i = PG, selectivity to LGA (S_{LGA}) is:

$$S_{LGA} = \frac{\dfrac{\text{moles of detected LGA}}{\text{initial moles of PG}}}{\dfrac{\text{moles of detected phenol}}{\text{initial moles of PG}}} \times 100\% = \frac{\text{moles of detected LGA}}{\text{moles of detected phenol}} \times 100\% \quad (7)$$

If i = G, selectivity to LGA (S_{LGA}) is:

$$S_{LGA} = \frac{\dfrac{\text{moles of detected LGA}}{\text{initial moles of glucose}}}{\dfrac{\text{initial moles of glucose} - \text{moles of HPLC detected glucose residue}}{\text{initial moles of glucose}}} \times 100\% = \frac{\text{moles of detected LGA}}{\text{initial moles of glucose} - \text{moles of HPLC detected glucose residue}} \times 100\% \quad (8)$$

2.5 Methyl-D-glucoside synthesis using glucose

The synthesis was carried out in a microwave reactor (Anton Paar Monowave 300), adapted from published procedures.[24] 90 mg of glucose, 21.5 mg of Amberlyst 15 (dry) and 2 mL of methanol were transferred into a 30 mL reaction tube, which was then heated to 130 °C, and held for 30 min under stirring at 1200 rpm. After cooling, the solution was diluted with DI water to a total volume 10 mL, and then the solid resin acid catalyst was removed using a 0.2 mm microfiber syringe filter (25 mm, VWR). The filtrate containing crude methyl-glucoside was analyzed for methyl-α-D-glucoside ("α-MG") and methyl-β-D-glucoside ("β-MG") content by ion-exclusion high-performance liquid chromatography (HPLC), using a Shimadzu Prominence SIL 20 system (Shimadzu Scientific Instruments, Inc., Columbia, MD, USA) equipped with an HPX-87H organic acid column (Bio-Rad, Hercules, CA, USA) and a refractive index detector (RID). The HPLC operation conditions were as follow: the column was operated at 42 °C, and 30 mM H_2SO_4 mobile phase was flowing through the column at 0.3 mL min^{-1}. Pure methyl-α-glucoside, methyl-β-glucoside, and D-glucose were used to calibrate the column.

Four μL of filtrate was transferred into a quartz tube and dried under vacuum to form the crude methyl-glucoside thin-film for the pyrolysis studies.

Glucose conversion in the synthesis step ($X_{G\_synthesis}$):

$$X_{G\_synthesis} = \frac{\text{initial moles of glucose} - \text{moles of HPLC detected glucose}}{\text{initial moles of glucose}} \times 100\% = \left(1 - \frac{\text{moles of HPLC detected glucose}}{\text{initial moles of glucose}}\right) \times 100\% \quad (9)$$

Methyl-glucosides yield ($Y_{\alpha\text{-MG}}$, $Y_{\beta\text{-MG}}$):

$$Y_{\alpha\text{-MG}} = \frac{\text{moles of HPLC detected } \alpha\text{-MG}}{\text{initial moles of glucose}} \times 100\% \quad (10)$$

$Y_{\beta\text{-MG}}$ was calculated by following similar equations.

Methyl-D-glucoside has also been synthesized from cellulose, filter paper and cotton (see ESI† for details).

2.6 Computation method

Quantum mechanical and statistical mechanical computations were performed using the Gaussian 09 program package (rev C.01).[25] The classical B3LYP functional was used with the electronic wave function expanded by the 6-31G(d,p) basis set. The Gibbs free energy was evaluated at 600 °C based on frequency analysis at the same level of theory. This level of theory is at a relatively lower level compared to some previous studies. To compare with published results, the Gibbs activation energy (the free energy difference between the highest-energy transition state and the lowest-energy reactant[26]) was computed to be 47.0 kcal mol^{-1} for LGA formation reaction, which was reasonably close to the value of 48.2 kcal mol^{-1} calculated from M06-2X/6-311+G (2df,p) level of theory[27] and the value of 52.5 kcal mol^{-1} from MP4(SDTD) single-point energy calculation based on geometries from B3LYP functional.[28]

3. Results and discussion

As an initial test, we synthesized a methyl substituted glucose (MG) by replacing the C_1 hydroxyl group of glucose (β-G and α-G mixture) with a methoxy group through Fischer glycosylation chemistry.[29] The resulting product contained 84 wt% methyl-D-glucoside, of which 44% was the β anomeric form. We heated the unpurified MG to 600 °C rapidly (flash pyrolysis ramp rate of ~20 000 °C s^{-1}), held it at 600 °C for 20 s, and analyzed the gas-phase effluent for pyrolysis products

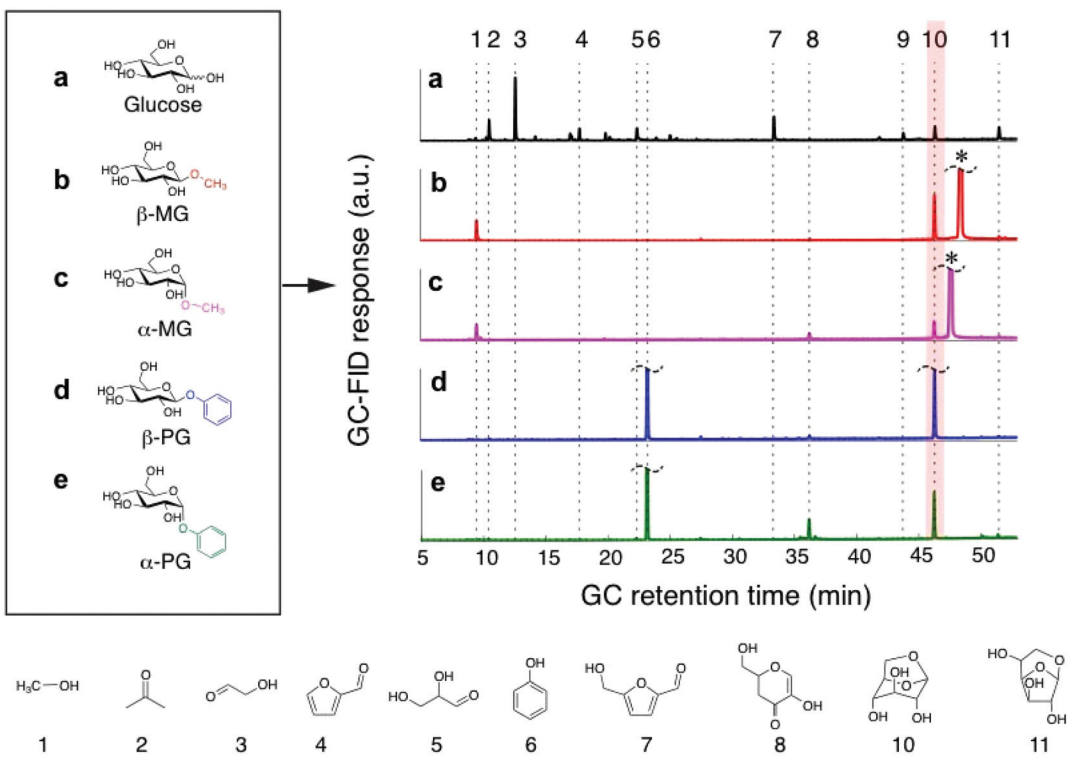

Fig. 1 Typical product distributions from glucose and glucoside pyrolysis at 600 °C. a–e, The multiplicity of products from (a) glucose pyrolysis is not found in the pyrolysis of (b) β-MG, (c) α-MG, (d) β-PG, or (e) α-PG. LGA product (compound #10) is highlighted. Details about the detected species are provided in Table S2.† The unreacted β-MG or α-MG precursor is marked with *. Flash pyrolysis reaction conditions: 600 °C, thin-film sample size = 32 μg, film thickness <10 μm (Fig. S1†), heating time of 20 s, carrier gas split ratio = 100 : 1.

Table 1 LGA conversion, yield, and selectivity values from glucose/glucoside pyrolysis at 600 °C. The bolded values were used in the pyrolysis experiments of Fig. 1

Compound	Split ratio	Probe heating time (second)	Interface temperature (°C)	Conversion (%)	Carbon yield (%)	Carbon selectivity (%)
β-G (decomposition temperature >152 °C)[31]	**100**	0.3	150	31	0.7 ± 0.6	2 ± 2
		0.4	150	76	0.9 ± 0.3	1 ± 0.4
		20	150	100	4 ± 0.2	4 ± 0.2
		20	**250**	100	3 ± 0.4	2 ± 0.4
β-MG (predicted boiling point = 389.1 ± 42.0 °C)[32]	**100**	0.5	250	7 ± 5	6 ± 5	81 ± 7
		1	250	11 ± 4	9 ± 2	83 ± 3
		20	**250**	17 ± 4	15 ± 4	84 ± 4
	50	20	250	21 ± 3	18 ± 3	84 ± 3
	20	20	250	40 ± 6	25 ± 5	63 ± 5
	10	20	250	47 ± 8	21 ± 6	48 ± 6
α-MG (predicted boiling point = 389.1 ± 42.0 °C)[32]	**100**	0.5	250	7 ± 3	4 ± 1	47 ± 3
		1	250	11 ± 4	5 ± 2	45 ± 5
		20	**250**	15 ± 5	7 ± 3	47 ± 7
	50	20	250	22 ± 5	10 ± 2	44 ± 6
	20	20	250	38 ± 2	13 ± 2	33 ± 4
	10	20	250	43 ± 5	12 ± 2	28 ± 4
β-PG (predicted boiling point = 482.1 ± 45.0 °C)[32]	**100**	0.1	250	9 ± 2	8 ± 3	92 ± 7
		0.5	250	18 ± 4	22 ± 4	92 ± 8
		20	**250**	23 ± 3	24 ± 4	93 ± 4
	50	20	250	28 ± 7	26 ± 11	92 ± 6
	20	20	250	39 ± 5	32 ± 5	83 ± 4
	10	20	250	54 ± 3	39 ± 3	72 ± 2
α-PG (predicted boiling point = 482.1 ± 45.0 °C)[32]	**100**	0.1	250	7 ± 4	12 ± 6	53 ± 8
		20	**250**	27 ± 8	4 ± 3	52 ± 3

(Fig. S2†). LGA selectivity from crude MG pyrolysis was ~64%, significantly higher than the experimentally determined ~2% selectivity from glucose pyrolysis.

We next carried out the pyrolysis of high-purity methyl-β-D-glucoside ("β-MG") and methyl-α-D-glucoside ("α-MG") under the same experimental conditions. We chose 600 °C for our studies, which is the higher end of the temperature range used in fast pyrolysis processes.[30] At lower pyrolysis temperatures, the selectivity for anhydrosugar increases and the selectivity for light oxygenates and permanent gases (CO_2 and CO) decreases (Table S1†). We adopted the thin-film pyrolysis technique of Dauenhauer and co-workers[22] to ensure the various sugar compounds did not experience concentration and temperature gradients during heating and to ensure consistent substrate conversion and LGA yield measurements. Fig. 1 shows representative chromatograms of the detected products from the pyrolysis of glucose, β-MG, and α-MG, as well as the β and α forms of phenyl-D-glucoside (PG). Pyrolysis of glucose led to dehydrated (LGA, 1,6-anhydro-β-D-glucofuranose, and HMF) and cracked (furfural, glyceraldehyde, glycolaldehyde, and acetone) products.[21–23] In comparison, pyrolysis of the substituted sugars led to mostly LGA (with methanol or phenol eliminated as a co-product) with decreased amounts of the other pyrolysis products.

A direct comparison of LGA yields provided an incomplete analysis, because the sugar compounds volatilized to different extents during pyrolysis treatment and did not undergo complete conversion (<60%). Instead, we quantified and compared

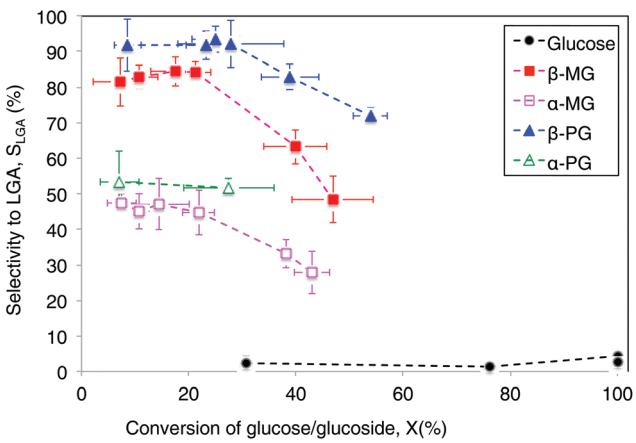

Fig. 2 LGA carbon selectivity-conversion analysis for the different sugar compounds. Each data point represents a minimum of 3 experiments, and the error bar is ±1 standard deviation. LGA selectivity values ($S_{LGA} = Y_{LGA} \div X_{sugar}$) were determined from yields Y_{LGA} measured at different sugar conversions (X_{sugar}). Conversion varied with carrier gas contact time at 600 °C.

LGA selectivity values, which accounts for incomplete conversion of the parent sugar (Table 1). Fig. 2 shows LGA selectivities from MG and PG pyrolysis, which readily exceeded 20%. In comparison, glucose pyrolysis had very low LGA selectivity (~1–4%) at all conversions observed (~30–100%). LGA selectivity from β-MG pyrolysis was in the 80–85% range at <20% con-

version and it decreased to ~48% near 50% conversion. Furan derivatives, light oxygenates, and char residue formed at higher conversions. α-MG pyrolysis showed a similar trend but selectivities were roughly half as much. Pyrolysis of the phenoxy-functionalized glucoses gave similar trends, with LGA selectivities measured as high as 93 ± 4% for β-PG. The highest LGA yield (39%) came from β-PG pyrolysis at 54% conversion (Table 1). At a sugar/glucoside conversion of 35%, LGA selectivity decreased in the following order: β-PG > β-MG > α-PG > α-MG ≫ glucose, showing the wide-ranging effects of substituent type and anomeric position.

We next studied the energy profiles of several key reaction pathways in β-G, β-MG, and β-PG pyrolysis, through DFT computation using the B3LYP functional and 6-31G(d,p) basis set. β-G can dehydrate into LGA and other anhydrosugars.[27,33] It can also mutarotate to the open-chain aldehyde form, which then goes through isomerization, retro-aldol cleavage, and dehydration reactions. Consistent with observations of numerous cracked products and low LGA selectivity, the ring-opening pathway for β-G pyrolysis has the lowest activation energy (P-1; 37.3 kcal mol^{-1}), followed by 1,6-dehydration to form LGA (P-2; 47.0 kcal mol^{-1}) and then by dehydration *via* β-eliminations (P-3 to P-5; ~59–71 kcal mol^{-1}) (Fig. 3).

Of particular interest are the lowest-barrier P-1 and P-2 pathways, which proceed through a common series of conformational changes of the pyranose ring. β-G flips from its stable chair conformation I into a boat structure III and then into an inverted chair V; the energy barriers are sufficiently small (~8 kcal mol^{-1}) such that these structures can be considered in pre-equilibrium with one another (Fig. 4a, Table S3†). Through a concerted set of bond cleavage and formation steps, structure V then converts into either the open-chain form *via* a six-atom-containing transition state VI[34] or into LGA *via* a four-atom-containing transition state vi.[35]

With the C_1 methoxy substituent, β-MG goes through P-1 and P-2 pathways *via* geometries very similar to those of β-G (Fig. 4b, Table S3†). The relative energies of the various states are essentially the same as in the β-G case, except for transition state VI. The activation barrier height increases substantially (by ~50 kcal mol^{-1} to 86.2 kcal mol^{-1}), leading to a ring-locking effect. Ring-opening becomes very difficult because the C_1 methoxy impedes the formation of the transitory six-atom cyclic structure. Whereas the 1s orbital of the H atom on O_1 of β-G has ample overlap with the O_6 sp^3 orbital (Fig. 6a), the methyl carbon sp^3 orbital on O_1 of β-MG does not (Fig. 6b). The methoxy group lowers the P-2 and P-3 barriers somewhat, and has no effect on the much higher P-4 and P-5 barriers. The observed high LGA selectivities directly result when 1,6-elimination becomes the energetically favored pathway after ring-opening is greatly suppressed.

The C_1 phenoxy substituent also impedes the pyranose ring from opening, with the P-1 barrier increasing to 85.0 kcal mol^{-1} (Fig. 4c and 6c; Table S3†). The P-2 barrier decreases by ~7 kcal mol^{-1}, reflecting an inductive effect of the phenyl group on the adjacent four-atom cyclic structure of transition state vi (Fig. 3 and 6d–f). The P-3 barrier decreases

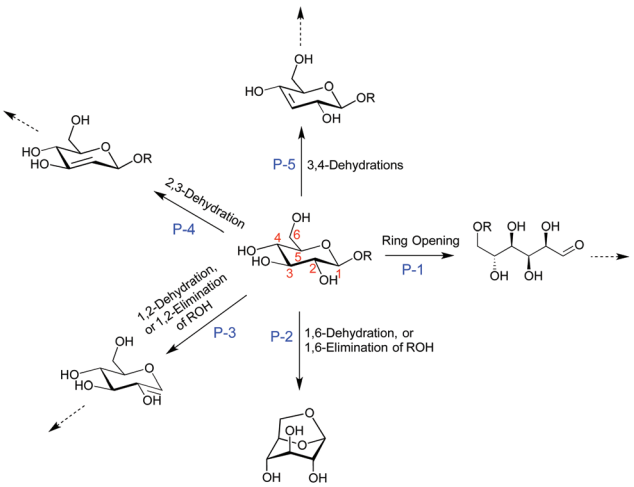

Pathway number	Transitory-cyclic structure in transition states	Bonds between R and Trasitory-cyclic structure	R=H ΔG (kcal/mol)	R=Me ΔG (kcal/mol)	R=Ph ΔG (kcal/mol)
P-1		0	37.3	86.2	85.0
P-2		1	47.0	46.6	40.3
P-3	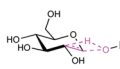	1	58.7	54.8	45.6
P-4	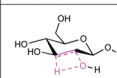	3	71.4	73.9	73.4
P-5	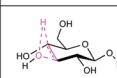	4	68.2	68.1	68.2

Fig. 3 Summary of key reactions and energy barriers in β-G, β-MG, and β-PG pyrolysis.

also (by ~13 kcal mol^{-1}) due to the inductive effect, generating 1,2-anhydro-β-D-glucopyranose that then isomerizes to LGA.[36] P-2 and P-3 pathways are kinetically favored over P-1, P-4, and P-5, contributing to the >90% LGA selectivities seen for β-PG pyrolysis.

We found that high LGA selectivities come primarily from the ring-locking effect by the C_1 group, even with the α anomers. Ring-opening of α-G, α-MG and α-PG proceeds through a different pathway involving a four-atom cyclic structure (Fig. S4 and S5†).[34] The activation energy increases from 44.9 kcal mol^{-1} to 76.2 and 70.1 kcal mol^{-1} when α-G is functionalized at the C_1 with methoxy and phenoxy groups, respectively.

LGA formation is more difficult when the C_1 OH/OR groups and C_6 hydroxymethyl groups are on opposite sides of the pyranose ring, with the α anomers going through a two-step carbene mechanism instead of the four-atom cyclic structure of the P-2 pathway.[27] The C_1 substituent abstracts the hydro-

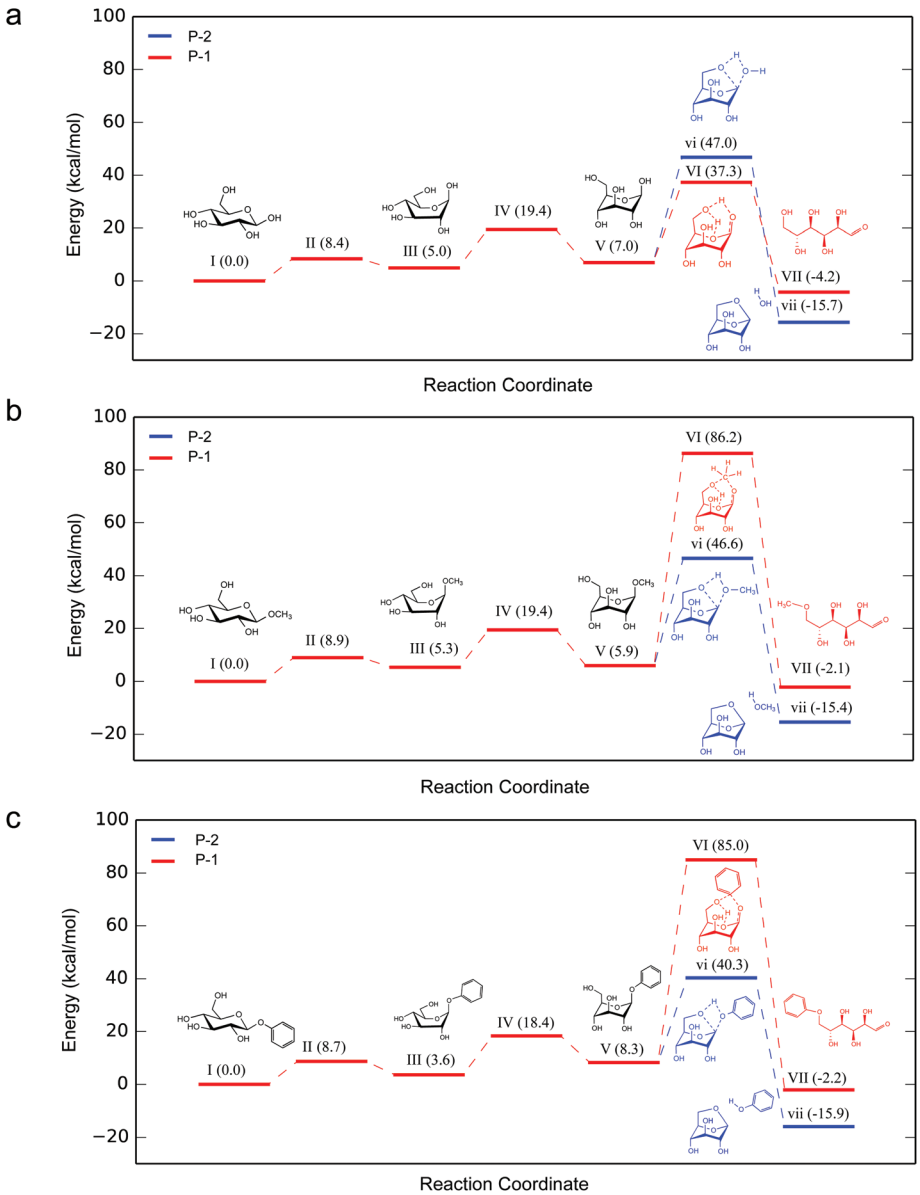

Fig. 4 Relative Gibbs free energy profiles for ring-opening (P-1) and LGA formation (P-2) pathways for (a) β-G, (b) β-MG and (c) β-PG pyrolysis at 600 °C. Structures vi and VI are the rate-determining transition states containing transient four-atom and six-atom cyclic structures, respectively. 3-D structures for (a) is shown in Fig. 5, for (b) and (c) are shown in Fig. S3.†

gen at C_1 to form a three-center transition state (structure b), resulting in a carbene intermediate (structure c); the latter then forms LGA *via* another three-center transition state (structure d). The LGA formation activation energy is relatively large, changing little after methoxy functionalization (from 66.2 to 69.0 kcal mol^{-1}) and decreasing after phenoxy functionalization (to 51.4 kcal mol^{-1}) (Fig. S4 and S5†). The lower LGA selectivities for α-MG and α-PG compared to β-MG and β-PG are due to the smaller activation barrier differences between ring-opening and 1,6-dehydration/elimination.

We observed the ring-locking effect in other C_1-functionalized monosaccharides (Fig. S6†). D-Mannose and D-galactose are common stereoisomers of D-glucose, in which their respective C_2 and C_4 OH groups are in the axial position. Pyrolysis of D-mannose (a mixture of α and β forms) led to 5% yield of the corresponding 1,6-anhydrosugar mannosan; in comparison, pyrolysis of methyl-α-D-mannoside led to 23% yield. Mannosan selectivities were 5% and 50%, respectively, after accounting for the difference in conversion. Similarly, pyrolysis of D-galactose and methyl-α-D-galactoside led to 5% and 11% galactosan yields and to selectivities of 5% and 23%.

Ring-locking can explain the higher LGA yields from longer cellulose chains than shorter ones. Cellulose pyrolysis generates LGA through depolymerization, in which the glycosidic bond between the C_1 of one sugar unit and the O_4 of an adjacent unit cleaves, and C_1 forms the intramolecular bond

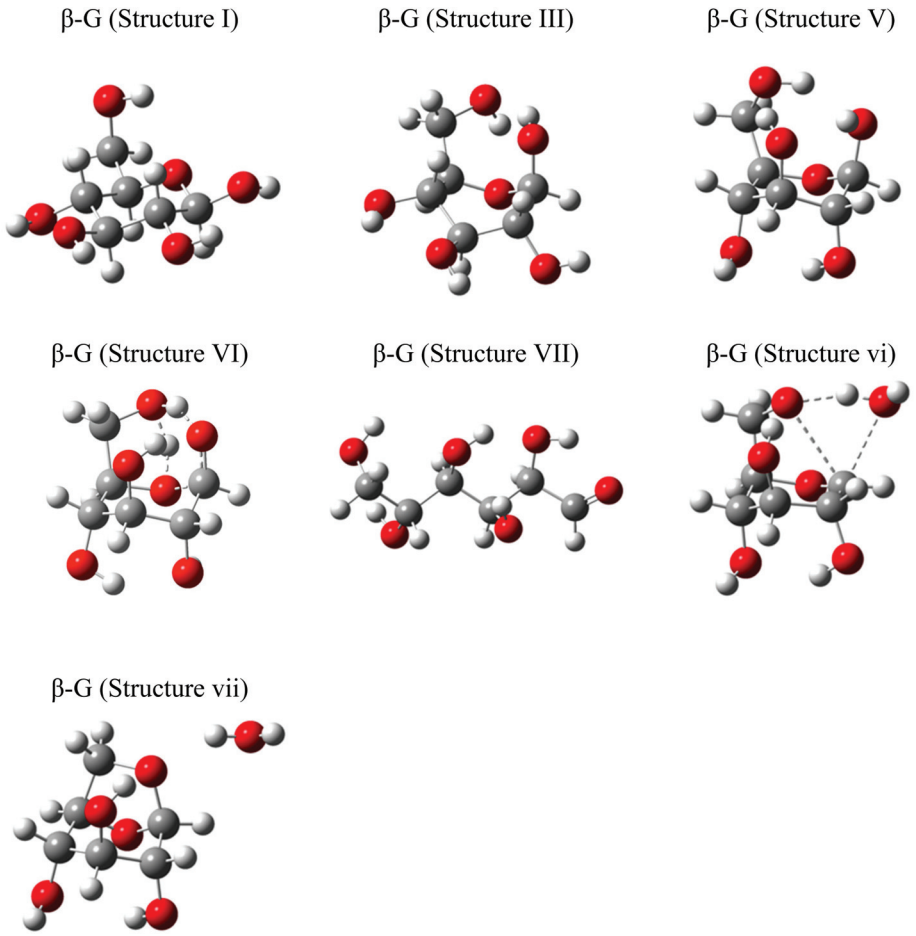

Fig. 5 Representative 3-D structures used in β-G ring opening and LGA formation pathway calculation, optimized at the B3LYP/6-31G(d,p) level of theory.

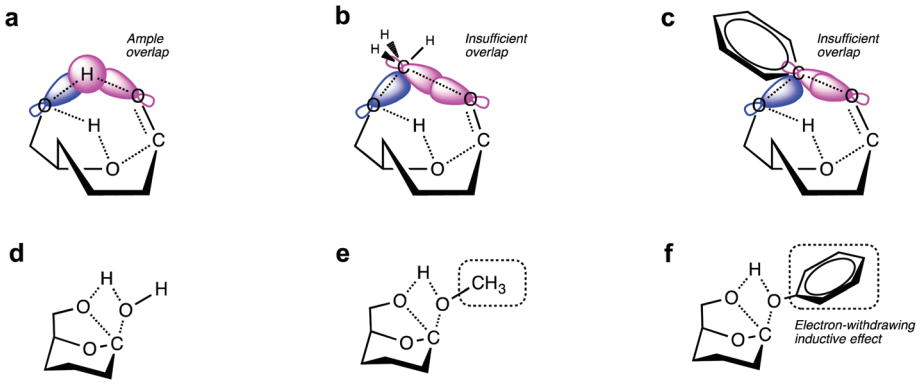

Fig. 6 Transition states showing the six-atom ring structure of (a) β-G, (b) β-MG, and (c) β-PG undergoing ring-opening, and the four-atom ring structures of (d) β-G, (e) β-MG, and (f) β-PG undergoing 1,6-dehydration/1,6-elimination.

with O_6. The adjacent unit at the C_1 position helps hinder ring-opening during depolymerization. It can also help explain how lignocellulose pyrolysis leads to higher LGA selectivities normalized to cellulose content (~48% for poplar wood v. ~27% for Avicel cellulose[37]). The cellulose fraction contains longer chains and has additional glycosidic linkages to hemicellulose and lignin, both of which contribute to the ring-locking effect.

We studied if cellulose solids can be pre-treated in such a way to improve LGA selectivity prior to pyrolysis. As a proof-of-concept, three different cellulose sources (microcrystalline cellulose, filter paper and cotton) were methoxylated into mixtures of α-MG and β-MG (Table S4†). Flash pyrolysis of the cellulose-derived methyl-D-glucoside crude gave a LGA yield of 15%. Pyrolysis of untreated cellulose gave a similar yield, though needing complete cellulose conversion. Accounting for the differences in conversion, LGA selectivities were 59% and 14% for treated and untreated cellulose, respectively. LGA selectivities (~50–60%) from the various methyl-D-glucoside crudes mapped between the selectivity-conversion curves for α-MG and for β-MG (Fig. S7†). Chemical modification of the carbohydrate source reduces the atom-inefficiency of cellulose pyrolysis.

4. Conclusions

Ring-locking is established as an efficient means to achieve substantially improved LGA selectivities from the pyrolysis of sugars. The presence of a substituent group at the anomeric carbon impedes pyranose ring-opening by raising the activation barrier of this pathway. The barrier for 1,6-elimination to form LGA decreases when the substituent group has a strong inductive effect. The multitude of reaction pathways in pyrolysis may be selectively redirected for substantially improved selectivities to anhydrosugars by simply ring-locking the anomeric carbon of the carbohydrates. Similar methods may also be applicable to monosaccharides with furanose ring structures.

Author contributions

L. C., M. S. W. and Z. C. Z. conceived the idea and designed the experiments. L.C. performed the pyrolysis experiments. L. C. and S. P. synthesized methyl-glucoside. J. M. Z. performed computations. B. E. B. collected SEM data. The manuscript was drafted by L. C. and M. S. W., with contributions and input from all authors.

Acknowledgements

This work was supported by the National Science Foundation (CBET-1153232, CBET-1247347 and CHE-1462434) and the CAS/SAFEA International Partnership Program for Creative Research Teams. L. Chen acknowledges support from the Kobayashi Fellowship Fund. We thank Prof. R. Gonzalez (Rice) for use of the high-performance liquid chromatography, and Dr J. M. Clomburg (Rice) for assistance. We also thank Dr P. Yan (DICP) and Mr Y. Gao (UT Austin) for experimental assistance, and Dr H. Qian (Rice), Dr H. Yu (DICP), Mr Y. Yin (Rice), and Mr Y. Zhou (Rice) for helpful discussions. We also thank additional support from KiOR, Inc.

Notes and references

1 R. C. Brown and T. R. Brown, *Biorenewable resources: engineering new products from agriculture*, John Wiley & Sons, 2013.
2 A. J. Ragauskas, C. K. Williams, B. H. Davison, G. Britovsek, J. Cairney, C. A. Eckert, W. J. Frederick, J. P. Hallett, D. J. Leak, C. L. Liotta, J. R. Mielenz, R. Murphy, R. Templer and T. Tschaplinski, *Science*, 2006, **311**, 484–489.
3 P. Anbarasan, Z. C. Baer, S. Sreekumar, E. Gross, J. B. Binder, H. W. Blanch, D. S. Clark and F. D. Toste, *Nature*, 2012, **491**, 235–239.
4 C. O. Tuck, E. Pérez, I. T. Horváth, R. A. Sheldon and M. Poliakoff, *Science*, 2012, **337**, 695–699.
5 M. J. Climent, A. Corma and S. Iborra, *Green Chem.*, 2011, **13**, 520.
6 C.-H. Zhou, X. Xia, C.-X. Lin, D.-S. Tong and J. Beltramini, *Chem. Soc. Rev.*, 2011, **40**, 5588–5617.
7 S. Czernik and A. V. Bridgwater, *Energy Fuels*, 2004, **18**, 590–598.
8 D. Radlein, in *Fast pyrolysis of biomass: a handbook*, ed. A. Bridgwater, 2002, pp. 205–241.
9 M. Bols, *Carbohydrate building blocks*, John Wiley & Sons, 1996.
10 C. J. Longley and D. P. C. Fung, in *Advances in Thermochemical Biomass Conversion*, 1994, vol. 2, pp. 1484–1494.
11 C. M. Lakshmanan, B. Gal-or and H. E. Hoelscher, *Ind. Eng. Chem. Prod. Res. Dev.*, 1969, **8**, 261–267.
12 J. P. Henschke, C. W. Lin, P. Y. Wu, W. S. Tsao, J. H. Liao and P. C. Chiang, *J. Org. Chem.*, 2015, **80**, 5189–5195.
13 US Department of Energy and E. E. and R. E. Energy, 2004.
14 B. R. T. Simoneit, J. J. Schauer, C. G. Nolte, D. R. Oros, V. O. Elias, M. P. Fraser, W. F. Rogge and G. R. Cass, *Atmos. Environ.*, 1999, **33**, 173–182.
15 F. Shafizadeh, R. H. Furneaux, T. G. Cochran, J. P. Scholl and Y. Sakai, *J. Appl. Polym. Sci.*, 1979, **23**, 3525–3539.
16 G. W. Huber, J. N. Chheda, C. J. Barrett and J. A. Dumesic, *Science*, 2005, **308**, 1446–1450.
17 H. Zhao, J. E. Holladay, H. Brown and Z. C. Zhang, *Science*, 2007, **316**, 1597–1600.
18 M. S. Holm, S. Saravanamurugan and E. Taarning, *Science*, 2010, **328**, 602–605.
19 C. Dellomonaco, J. M. Clomburg, E. N. Miller and R. Gonzalez, *Nature*, 2011, **476**, 355–359.
20 M. S. Mettler, A. D. Paulsen, D. G. Vlachos and P. J. Dauenhauer, *Green Chem.*, 2012, **14**, 1284.
21 P. R. Patwardhan, J. A. Satrio, R. C. Brown and B. H. Shanks, *J. Anal. Appl. Pyrolysis*, 2009, **86**, 323–330.
22 M. S. Mettler, S. H. Mushrif, A. D. Paulsen, A. D. Javadekar, D. G. Vlachos and P. J. Dauenhauer, *Energy Environ. Sci.*, 2012, **5**, 5414.
23 Y.-C. Lin, J. Cho, G. A. Tompsett, P. R. Westmoreland and G. W. Huber, *J. Phys. Chem. C*, 2009, **113**, 20097–20107.
24 Y. Yang, M. M. Abu-Omar and C. Hu, *Appl. Energy*, 2012, **99**, 80–84.

25 M. J. Frisch, G. W. Trucks, H. B. Schlegel, G. E. Scuseria, M. A. Robb, J. R. Cheeseman, G. Scalmani, V. Barone, B. Mennucci, G. A. Petersson, H. Nakatsuji, M. Caricato, X. Li, H. P. Hratchian, A. F. Izmaylov, J. Bloino, G. Zheng, J. L. Sonnenberg, M. Hada, M. Ehara, K. Toyota, R. Fukuda, J. Hasegawa, M. Ishida, T. Nakajima, Y. Honda, O. Kitao, H. Nakai, T. Vreven, J. A. Montgomery Jr., J. E. Peralta, F. Ogliaro, M. Bearpark, J. J. Heyd, E. Brothers, K. N. Kudin, V. N. Staroverov, R. Kobayashi, J. Norman, K. Raghavachari, A. Rendell, J. C. Burant, S. S. Iyengar, J. Tomasi, M. Cossi and N. Rega, 2009.
26 S. Kozuch and S. Shaik, *Acc. Chem. Res.*, 2011, **44**, 101–110.
27 H. B. Mayes, M. W. Nolte, G. T. Beckham, B. H. Shanks and L. J. Broadbelt, *ACS Sustainable Chem. Eng.*, 2014, **2**, 1461–1473.
28 T. Hosoya, H. Kawamoto and S. Saka, *J. Anal. Appl. Pyrolysis*, 2009, **84**, 79–83.
29 F. W. Lichtenthaler, in *Ullmann's Encyclopedia of Industrial Chemistry*, 2010, pp. 617–642.
30 P. Basu, *Biomass gasification and pyrolysis: practical design and theory*, Academic press, 2010.
31 M. Hurtta, I. Pitkänen and J. Knuutinen, *Carbohydr. Res.*, 2004, **339**, 2267–2273.
32 ACD/Percepta, Adv. Chem. Dev. Inc., Toronto, Canada, 2014. http//www.acdlabs.com.
33 R. Vinu and L. J. Broadbelt, *Energy Environ. Sci.*, 2012, **5**, 9808.
34 V. Seshadri and P. R. Westmoreland, *J. Phys. Chem. A*, 2012, **116**, 11997–12013.
35 T. Hosoya, Y. Nakao, H. Sato, H. Kawamoto and S. Sakaki, *J. Org. Chem.*, 2009, **74**, 6891–6894.
36 R. S. Assary and L. A. Curtiss, *ChemCatChem*, 2012, **4**, 200–205.
37 J. Piskorz, D. S. A. G. Radlein, D. S. Scott and S. Czernik, *J. Anal. Appl. Pyrolysis*, 1989, **16**, 127–142.